Published in final edited form as:
J Steroid Biochem Mol Biol. 2013 November ; 138: 81–89. doi:10.1016/j.jsbmb.2013.03.012.

1, 25 Dihydroxyvitamin D Regulation of Glucose Metabolism in Harvey-*ras* Transformed MCF10A Human Breast Epithelial Cells

Wei Zheng[1], **Fariba Tayyari**[2], **G. A. Nagana Gowda**[2,3], **Daniel Raftery**[2,3], **Eric S. McLamore**[4], **Jin Shi**[4,5], **D. Marshall Porterfield**[4,5,6,7], **Shawn Donkin**[1], **Brian Bequette**[8], and **Dorothy Teegarden**[1]

[1]Interdepartmental Nutrition Program, Purdue University, West Lafayette, IN 47906.

[2]Department of Chemistry, Purdue University, West Lafayette, IN 47906.

[4]Birck-Bindley Physiological Sensing Facility, Purdue University, West Lafayette, IN 47906.

[5]Weldon School of Biomedical Engineering, Purdue University, West Lafayette, IN 47906.

[6]Department of Agricultural and Biological Engineering, Purdue University, West Lafayette, IN 47906.

[7]Department of Horticulture and Landscape Architecture, Purdue University, West Lafayette, IN 47906.

[8]Department of Animal and Avian Sciences, University of Maryland, College Park, MD.

Abstract

This study was designed to investigate the impact of 1,25 dihydroxyvitamin D ($1,25(OH)_2D$) on glucose metabolism during early cancer progression. Untransformed and *ras*-oncogene transfected (*ras*) MCF10A human breast epithelial cells were employed to model early breast cancer progression. $1,25(OH)_2D$ modified the response of the *ras* cells to glucose restriction, suggesting $1,25(OH)_2D$ may reduce the *ras* cell glucose addiction noted in cancer cells. To understand the $1,25(OH)_2D$ regulation of glucose metabolism, following four-day $1,25(OH)_2D$ treatment, metabolite fluxes at the cell membrane were measured by a nanoprobe biosensor, [$^{13}C_6$]glucose flux by ^{13}C-mass isotopomer distribution analysis of media metabolites, intracellular metabolite levels by NMR, and gene expression of related enzymes assessed. Treatment with $1,25(OH)_2D$ reduced glycolysis as flux of glucose to 3-phosphoglycerate was reduced by 15% ($P = 0.017$) and

Corresponding Author: Dorothy Teegarden, Purdue University, 700 W. State Street, West Lafayette, 47907; teegarden@purdue.edu.
[3]Current address: Mitochondria and Metabolism Center, Department of Anesthesiology and Pain Medicine, University of Washington, Seattle, WA 98109.
Wei Zheng: zheng38@purdue.edu; Fariba Tayyari: ftayyari@purdue.edu; G.A. Nagana Gowda: ngowda@uw.edu; Daniel Raftery: draftery@uw.edu; Eric S. McLamore: emclamor@ufl.edu; D. Marshall Porterfield: porterf@purdue.edu; Brian Bequette: bbequett@umd.edu; Shawn Donkin: sdonkin@purdue.edu

Conflict of Interest Statement:

No potential conflicts of interest were disclosed by the authors.

32% (P < 0.003) in MCF10A and *ras* cells respectively. In the *ras* cells, 1,25$(OH)_2$D reduced lactate dehydrogenase activity by 15% (P < 0.05) with a concomitant 10% reduction in the flux of glucose to lactate (P = 0.006), and reduction in the level of intracellular lactate by 55% (P = 0.029). Treatment with 1,25$(OH)_2$D reduced flux of glucose to acetyl-coA 24% (P = 0.002) and 41% (P < 0.001), and flux to oxaloacetate 34% (P = 0.003) and 33% (P = 0.027) in the MCF10A and *ras* cells, respectively, suggesting a reduction in tricarboxylic acid (TCA) cycle activity. The results suggest a novel mechanism involving the regulation of glucose metabolism by which 1,25$(OH)_2$D may prevent breast cancer progression.

Keywords

vitamin D; cancer prevention; breast cancer; glucose; energy metabolism; *ras*; 1, 25 dihydroxyvitamin D

1. Introduction

Breast cancer is the second leading cancer among women in the US, with devastating consequences physically, emotionally and financially. Approximately 15% of cancer deaths in women result from breast cancer [1]. A growing body of evidence suggests that vitamin D may play a role in preventing the development of breast cancer [2-6]. For example, areas with higher latitudes and lower solar radiation, which leads to lower vitamin D synthesis in the skin, have increased mortality from breast cancer [3]. Substantial literature also supports that better vitamin D status is associated with reduced risk of breast cancer [2, 4, 5], but the mechanism is not clear.

The major circulating form of vitamin D, 25(OH)D, produced in the liver, is hydroxylated by 1α-hydroxylase in the kidney to the bioactive form of vitamin D, 1α, 25-dihydroxyvitamin D (1,25$(OH)_2$D). Research supports that 1,25$(OH)_2$D has anti-neoplastic effects in colon, prostate, ovarian and breast cancer [2, 7]. 1,25$(OH)_2$D is proposed to prevent cancer progression through the modulation of expression of many genes involved in cell growth, apoptosis, angiogenesis and immune responses [8, 9]. However, the mechanisms in progression of breast cancer in particular and the effect of oncogenes on the action of 1,25$(OH)_2$D in early cancer progression are not fully understood.

One of the critical shifts in progression to tumorigenesis is in cellular energy metabolism [10]. The metabolic switch that occurs during carcinogenesis (including the Warburg effect) is a general characteristic of proliferating cells [10, 11], which may lead to increased glucose metabolism and the dependence of cells on glucose (addiction) [12]. Proliferating cells not only require energy, but also nutrients in amounts greater than their bioenergetic needs in order to provide biosynthetic precursors, such as lipids, proteins and nucleic acids, for continued cell proliferation [11]. In nonproliferating cells, most of the pyruvate generated by glycolysis can be completely metabolized through the TCA cycle to produce large amount of ATPs in the presence of oxygen. In contrast, in rapidly proliferating cells and cancer cells, there is an increased glucose uptake and a shift of the pyruvate oxidative phosphorylation in the mitochondria towards a more rapid aerobic glycolysis, even in a normoxic environment, as described in the classic Warburg effect [10, 11]. This decrease in

glucose flux into the TCA cycle, which is controlled by the key enzyme pyruvate dehydrogenase (PDH) and its inhibitory kinase pyruvate dehydrogenase kinase (PDK), is another key feature of the classic Warburg effect [13, 14]. These alterations in glucose metabolism result in dramatically reduced production of ATP and increased conversion of pyruvate to lactate, which allows glycolysis to continue by regenerating NAD+. The resulting lactate may also serve as an energy source for tumor cells [15]. Further, the rate of glucose metabolism in this metabolic switch increases dramatically. In fact, cancer cells divert about 10% of the glucose into biosynthetic pathways upstream of pyruvate production [11], which provides an advantage to cancer cells by favoring utilization of the most abundant energy and carbon sources. For example, glucose metabolism yields ribose for nucleic acid synthesis and NADPH through pentose phosphate pathway (PPP) while greater glycolysis provides intermediates to maintain anaplerosis and supply of biosynthetic intermediates [11] for the synthesis of fatty acids, nucleic acids and amino acids for continued cellular growth and replication. Further, the high rate of NADPH generation also aids in the anti-oxidant defense mechanisms of the cancer cells. Thus, deprivation of glucose can induce oxidative stress and other defects in metabolism which leads to cancer cell apoptosis [16, 17]. Inhibitors of glucose transporters and glycolysis have been implemented as effective anticancer treatments and can also sensitize the tumor cells to other chemotherapeutic drugs [18, 19]. Unlike in untransformed proliferating cells, the metabolic reprogramming in cancer cells is controlled by growth factor independent, chronic activation of the proliferative pathways [11]. Previous studies demonstrate that the increase in glycolysis in the Warburg effect in cancer cells is at least in part mediated by increases in multiple enzymes in the glycolytic pathway [19]. In order to establish strategies for cancer prevention by vitamin D, it is critical to determine whether and through which mechanism it regulates energy metabolism in normal cells and prevents the metabolic switch in cells containing oncogenes such as the activated *ras* gene.

The *ras* proto-oncogene is frequently mutated in cancer and affects a variety of tumorigenic processes including proliferation [20, 21]. It encodes four distinct RAS proteins (HRAS, NRAS, KRAS4A and KRAS4B) which are small GTPases essential for the signal transduction induced by numerous growth factors to stimulate cell proliferation. The oncogenic RAS promotes both pro-growth and inhibits anti-growth signals in a growth factor independent manner [20]. The oncogenic RAS may also aid in metabolic reprogramming towards glycolysis in transformed cells. Previous studies show that K-*ras* transformed fibroblast cells have increased glycolytic activity and altered cellular glucose metabolism [22]. Furthermore, research supports that vitamin D receptor (VDR) transcriptional activity is down-regulated in the presence of *ras* oncogene [23-25], potentially disrupting the effect of $1,25(OH)_2D$ to inhibit tumorigenesis. Therefore, it is important to study the effect of $1,25(OH)_2D$ on cellular energy metabolism in *ras* oncogene transformed cells.

The effect of $1,25(OH)_2D$ on cellular glucose metabolism and its biological outcomes in early breast cancer progression have not been studied. The purpose of the current study was to investigate the effect of $1,25(OH)_2D$ regulation of cellular glucose energy metabolism in human breast epithelial cells with and without the Harvey-*ras* oncogene. The hypothesis of

the current study is that $1,25(OH)_2D$ shifts glucose utilization towards reduced glycolysis and lactate production as well as reduced flux through the TCA cycle in *Harvey-ras* transfected breast epithelial cells but not in untransformed cells. These results will contribute to the understanding of $1,25(OH)_2D$ action on breast tissue during mammary carcinogenesis.

2. Materials and methods

2.1. Chemicals and reagents

The$1,25(OH)_2D$ was purchased from Biomol (Plymouth Meeting, PA). Dulbecco's modified Eagle medium: Nutrient Mixture F-12 (DMEM/F12) media, horse serum, trypsin and penicillin/streptomycin were obtained from Life Technologies, Gibco-BRL (Rockville, MD). Cholera toxin was purchased from Calbiochem (Darmstadt, Germany). Bicinchoninic acid (BCA) protein assay reagents were obtained from Pierce (Rockford, IL). Protease inhibitor cocktail, trypan blue, insulin, epidermal growth factor, and hydrocortisone were from Sigma (St. Lois, MO). Tris-HCl Bio-Rad Ready Gels were purchased from Bio-Rad Laboratories (Hercules, CA). The QuantiChrom Lactate Dehydrogenase Kit was from BioAssay Systems (Hayward, CA). All reagents for gas chromatography-mass spectrometry (GCMS) analyses were from Pierce (Rockford, IL). D-[$^{13}C_6$]Glucose was purchased from Cambridge Isotope labs (Woburn, MA). Mass spectrometry analysis confirmed its chemical and isotopic purity (92.7% [$^{13}C_6$]glucose and 6.9% [$^{13}C_5$]glucose).

2.2. Cell culture

MCF10A human breast epithelial cells and MCF10A cells stably transfected with the Harvey *ras* oncogene (MCF10A-*ras* cells) were a gift from Dr. Michael Kinch, Purdue University. MCF10A and MCF10A-*ras* cells were cultured in the standard media recommended for these cells [26], the Dulbecco's Modified Eagle Medium: Nutrient Mixture F-12 (DMEM/F12, 1:1) containing 17 mM glucose, and supplemented with 5% horse serum, 10 mg/L insulin, 20 μg/L epidermal growth factor, 50 μg/L cholera toxin, 50 mg/L hydrocortisone, 100 units/ml penicillin, and 0.1 mg/mL streptomycin in a humidified environment at 37°C with 5% CO_2. DMEM/F12 (1:1) containing 17 mM glucose was used in all assays except for the MTT and flow cytometry analysis as indicated in Figure 1. Cells were maintained in fresh media changed every 24 hours during the 4-day treatment period. The $1,25(OH)_2D$ treatment was delivered to cells in 100% ethanol at a final ethanol concentration <1%.

2.3. MTT cell proliferation assay

Cells were cultured in media containing 5 mM glucose and the media changed that containing different glucose levels (0.1, 1, 5, and 17 mM) for the last 24 hours. Relative viable cell levels were determined by the MTT assay according to the manufacturer's recommendations. Results were expressed as the relative absorbance compared to that in the vehicle treated cells in media containing 5 mM glucose.

2.4. Cell cycle analysis

From each sample, 1×10^6 cells were harvested with phosphate buffered saline (PBS) in single cell suspension. Cells were fixed with ice cold ethanol, pretreated with 0.2 mg/ml

Rnase A, and stained with 10 ug/ml propidium iodide. Flow cytometry analysis was performed with a Beckman Coulter FC500 flow cytometer equipped with 488 nm laser. The results were analyzed using FlowJo (Tree Star, Inc., Ashland, OR). Results were expressed as percentage of total cells arrested in G1 phase in the cell cycle.

2.5. LDH Assay

Cells were washed with calcium and magnesium free-phosphate buffered saline (CMF-PBS) and harvested on ice into buffer containing 100 mmol/L potassium phosphate (pH 7.0), 2 mmol/L EDTA, and 1% protease inhibitor cocktail and phosphatase inhibitor cocktail. Cells were briefly sonicated and cell debris was removed by centrifugation at 12,000 RPM for 15 min at 4°C. Colorimetric kinetic determination of lactate dehydrogenase (LDH) activity in the cell lysate was measured using the QuantiChrom Lactate Dehydrogenase Kit (DLDH-100, BioAssay Systems). Values are expressed as LDH activity/total protein (specific activity).

2.6. Metabolomics

Cells were washed with CMF-PBS and harvested on ice into doubly distilled water. Cell lysates were obtained by freezing the cells in dry ice/ethanol bath for 5 min, and thawing them in 37°C water bath for 1 min. Cell debris was pelleted by centrifugation at 12,000 RPM for 2 min at 4°C. The supernatant was collected for metabolite profiling analysis using nuclear magnetic resonance (NMR) spectroscopy and mass spectrometry (MS) as described previously [27-29]. Metabolite levels were normalized to protein content.

2.7. ^{13}C-Metabolite flux analysis

Two hours prior to cell harvest, media were changed to fresh media with equal concentrations of unlabelled and $^{13}C_6$-labeled glucose, and collected after incubation for two hrs. Cells were rinsed with CMF-PBS, harvested on ice into lysis buffer and briefly sonicated. The cell lysates were saved for protein and DNA analysis, and media was used to determine the ^{13}C-mass isotopomer distribution analysis of metabolites and amino acids using GCMS. Briefly, 0.2 mL of sulfosalicylic acid (50% w:v) was added to 1 mL of media. The acid-supernatant was desalted by cation (AG 50W-X8, H+ form) exchange, and amino acids and lactate eluted with 2 mol/L NH_4OH followed by water. The frozen eluate was lyophilized to dryness, and amino acids converted to their *t*-butyldimethylsilyl derivative prior to GCMS (HP 5973N Mass Selective Detector, Agilent, Palo Alto, CA). Fragment ions containing all carbons of an analyte (lactate, pyruvate, serine, aspartate and glutamate) were monitored under electron impact mode. Normalized crude ion abundances of the enriched analytes were corrected for the measured natural abundance of stable isotopes present in the original molecule and that contributed by the derivative using the matrix approach [30].

Flux calculations were based on tracer:tracee ratios (TTR) in the form mol ^{13}C-isotopomer (M+n) per 100 mol ^{12}C analyte (M+0), where n equals the number of ^{13}C-labelled carbons in the analyte, e.g. [M+1], [M+2] and [M+3]lactate. Catabolism of [$^{13}C_6$]glucose via the glycolytic pathway results in distinctive ^{13}C-labelling patterns in metabolites that provide information on the contributions of glucose to pathways fluxes and the activity of the enzymatic pathways through which the ^{13}C-skeleton traversed [31]. Under steady-state

conditions, catabolism of [$^{13}C_6$]glucose leads to [M+3]pyruvate and then [M+3]lactate. Thus, the contribution of glucose to the flux of pyruvate and lactate can be assessed from the ratios [M+3]pyruvate to [M+6]glucose and [M+3]lactate to [M+6]glucose, respectively. Further, since lactate derives from cytosolic pyruvate, appearance of [M+1] and [M +2]lactate represents metabolism of [$^{13}C_6$]glucose via the PPP. Thus, the ratio [M+3]lactate to [M+1]lactate provides a crude measure of the relative activities of glycolysis versus the PPP.

Metabolism of the [M+3]pyruvate isotopomer via pyruvate carboxylase (PC) introduces the [M+3]oxaloacetate isotopomer into the Krebs cycle which, subsequently, reaches a metabolic equilibrium with its transamination partner [M+3]aspartate [32]. Similarly, [M +3]oxaloacetate eventually leads to formation of [M+3]α-ketoglutarate, which is in metabolic equilibrium with its transamination partner [M+3]glutamate. Alternatively, the [M +3]pyruvate isotopomer can be metabolized via pyruvate dehydrogenase (PDH) to yield [M +2]acetyl-CoA and thence [M+2]α-ketoglutarate and [M+2]glutamate. However, the [M +2]glutamate also arises as a consequence of the equilibrium reaction between oxaloacetate and fumarate. This metabolic cycle yields an equal mixture of 2 positional isotopomers of [M+3]oxaloacetate, one labeled in carbons 1-3 and the other in carbons 2-4. In consequence, because the decarboxylation step between citrate and α-ketoglutarate leads to the loss of carbon 1 of oxaloacetate (i.e. half of [M+3]oxaloacetate contributes to [M+2]α-ketoglutarate enrichment), a correction to the [M+2]glutamate enrichment was made. In consequence, the contribution of glucose to oxaloacetate and acetyl-CoA fluxes can be assessed by the ratios [M+3]aspartate to [M+6]glucose and corrected [M+2]glutamate to [M+6]glucose, respectively. Furthermore, the relative activities of PDH vs. PC can be assessed from the ratio of [M+2]glutamate to [M+3]glutamate.

2.8. Membrane metabolite fluxes

A highly sensitive and selective glucose oxidase-based micro biosensor decorated with platinum nanoparticle was employed in self-referencing mode to measure real-time physiological glucose flux across the cell membrane [33]. Self-referencing involves oscillation of a single microsensor via computer-controlled stepper motors within the concentration boundary layer near cells/tissues. This non-invasive technique provides direct measurement of trans-membrane analyte flux, and is reviewed in detail by McLamore and Porterfield [34].

2.9. RNA isolation and analysis

RNA was isolated with TriReagent (Molecular Research Center, Cincinnati, OH) following the manufacturer's instructions. Reverse transcription of total RNA was performed using MMLV reverse transcriptase (Promega, Madison, WI). Real-time quantitative PCR was performed using the Brilliant II SYBR Green QPCR Master Mix (Agilent, Santa Clara, CA). The mRNA abundances of enzymes involved in glucose metabolism were determined from the threshold cycle (Ct) value. The mRNA expression was normalized to 18S expression and results were expressed as arbitrary units. The primers used are shown Table 1.

2.10. Statistical Analysis

Values are presented as mean ± SEM. Results are expressed compared to the vehicle within the same cell line, by the Student's t-tests (LSD), or by analysis of variance (ANOVA), with $P<0.05$ considered statistically significant.

3. Results

3.1. 1,25(OH)$_2$D reduces glucose addiction

The impact of 1,25(OH)$_2$D treatment on glucose addiction of the cells was examined by MTT cell proliferation assay and flow cytometry analysis. 1,25(OH)$_2$D reduced the number of MCF10A-*ras* cells but not MCF10A cells by 44% and 37% in media containing 5 and 17 mM glucose, respectively (Figure 1A). Glucose restriction at 0.1 and 1 mM reduced the number of MCF10A-*ras* cell by 60% and 39%, respectively (Figure 1A), indicating the cell dependence on glucose (addiction). However, 1,25(OH)$_2$D prevented the reduction in cell number at 1 mM glucose, suggesting 1,25(OH)$_2$D may reduce the cell glucose addiction of MCF10A-*ras* cells. Consistent with these results, cell cycle analysis by flow cytometry showed that 1,25(OH)$_2$D increased the percentage of MCF10A-*ras* cells in G1 phase from 63% to 70% and from 48% to 64% in 1 and 5 mM glucose, respectively (Figure 1B). Glucose restriction at 1 mM caused 30% more *ras* cells in G1 phase, but 1,25(OH)$_2$D treatment prevented the increase in G1 arrest (Figure 1B), which suggest that 1,25(OH)$_2$D may reduce glucose addiction. These results suggest 1,25(OH)$_2$D reduces the *ras* cell glucose addiction, supporting the regulation of glucose metabolism by 1,25(OH)$_2$D during early cancer progression.

3.2. 1,25(OH)$_2$D reduces glucose uptake and aerobic glycolysis

To investigate the impact of 1,25(OH)$_2$D on glucose uptake and glycolytic activity, MCF10A and MCF10A-*ras* cells were treated with vehicle or 1,25(OH)$_2$D for 4 days. Glucose influx across the cell membrane in response to increasing concentrations of glucose in the media was measured employing a bio-nanosensor [33]. There was a glucose concentration dependent increase in glucose influx for both 1,25(OH)$_2$D and vehicle treated MCF10A-*ras* cells (Figure 2A). At high glucose concentration (15 mM), glucose influx was reduced in cells treated with 1,25(OH)$_2$D compared to cells treated with vehicle ($P<0.05$). The effects of 1,25(OH)$_2$D on the expression of proteins and enzymes in the glycolytic pathway were also examined. Glucose transporter 1 (GLUT1) is the major glucose transporter expressed in the human breast epithelial cells. Results showed that mRNA expression of GLUT1 was reduced by 28% in the 1,25(OH)$_2$D treated MCF10A cells, but not for the MCF10A-*ras* cells compared to vehicle treated cells (Figure 2B), suggesting that the reduction of glucose uptake by 1,25(OH)$_2$D treated MCF10A-*ras* cells may not be mediated through a decrease in expression of GLUT1. In contrast, mRNA expression of hexokinase 2 (HK2), the enzyme mediating the first step of phosphorylation of glucose during glycolysis, was induced by 23% by 1,25(OH)$_2$D in MCF10A cells, but not MCF10A-*ras* cells (Figure 2C). Phosphoglycerate kinase 1 (PGK1) catalyzes the seventh step of glycolysis, where 1,3-bisphosphoglycerate is converted to 3-phosphoglycerate. 1,25(OH)$_2$D reduced the expression of PGK1 by 13% in MCF10A cells and there was a trend towards a decrease in MCF10A-*ras* cells (Figure 2D). Consistent with the latter, results from the

analysis of the flux contribution of $^{13}C_6$-labeled glucose to glycolytic intermediates showed that following 1,25(OH)$_2$D treatment, the contribution of glucose to 3-phosphoglycerate flux was reduced by 15% and 32% compared to vehicle in MCF10A and MCF10A-*ras* cells, respectively (Figure 2E). Moreover, the proportion of pyruvate flux from glucose was reduced by 9% in MCF10A-*ras* cells, but was not altered in MCF10A cells (Figure 2F), suggesting that glycolysis is reduced by 1,25(OH)$_2$D only in the MCF10A-*ras* cells.

Phosphoenolpyruvate (PEP) is a glycolytic intermediate converted to pyruvate via pyruvate kinase (PK) in the rate-limiting final step of glycolysis. But metabolic profiling of MCF10A and MCF10A-*ras* cells showed that compared to vehicle treated cells, intracellular levels of PEP was ~1.5-fold higher in MCF10A and MCF10A-*ras* cells treated with 1,25(OH)$_2$D (Figure 2G). However, the mRNA expression of pyruvate kinase M2 (PKM2) (Figure 2H), the predominant isoform of PK expressed in the MCF10A cells that promotes metabolic programming for tumor growth [35], was not different in vehicle and 1,25(OH)$_2$D treated MCF10A and MCF10A-*ras* (Figure 2H). Further, total activity of PK was not affected by 1,25(OH)$_2$D treatment (Figure 2I), suggesting that the accumulation of PEP is not a result of reduced PK activity by 1,25(OH)$_2$D. Collectively, these data support that 1,25(OH)$_2$D may reduce glucose uptake and glycolytic activity in MCF10A-*ras* cells at an early stage of cancer progression.

3.3. 1,25(OH)$_2$D reduces lactate production

One of the components of the Warburg effect in tumor cells is the increased conversion of pyruvate to lactate. To determine whether 1,25(OH)$_2$D impacts lactate production, the activity of lactate dehydrogenase (LDH) was examined in MCF10A and MCF10A-*ras* cells following 4 days of 1,25(OH)$_2$D treatment. There was a 15% reduction in LDH activity by 1,25(OH)$_2$D in MCF10A-*ras* cells, but not in MCF10A cells, compared to vehicle (Figure 3A). Consistent with the reduction in LDH activity, 1,25(OH)$_2$D reduced the intracellular lactate by 55% in MCF10A-*ras* cells, but not in MCF10A cells (Figure 3B). $^{13}C_6$-Glucose kinetics also showed that 1,25(OH)$_2$D reduced the contribution of glucose to lactate flux by 10% in MCF10A-*ras* cells, but not in MCF10A cells (Figure 3C). These results suggest that 1,25(OH)$_2$D may reduce lactate production in MCF10A-*ras* cells during cancer progression, but not in untransformed MCF10A cells.

3.4. 1,25(OH)$_2$D reduces TCA cycle activity

The impact of 1,25(OH)$_2$D on TCA cycle activity in cells in progression to tumor were examined. The contribution of glucose to TCA cycle intermediate fluxes was assessed. Following 4 days of 1,25(OH)$_2$D treatment, there were 24% and 41% reductions in the contribution of glucose to acetyl-CoA flux in MCF10A and MCF10A-*ras* cells, respectively, compared to vehicle (Figure 4A). Further, 1,25(OH)$_2$D treatment reduced the contribution of glucose to oxaloacetate flux by 33% and 34% (Figure 4B) in MCF10A cells and MCF10A-*ras* cells, respectively, suggesting an overall reduction of glucose metabolism in the TCA cycle. Consistent with these results, the ^{13}C-tracer kinetics indicated a reduction in pyruvate dehydrogenase (PDH) activity by 22% and 24% in MCF10A and MCF10A-*ras* cells treated with 1,25(OH)$_2$D (Figure 4C). In addition, metabolic profiling showed there was a 29% reduction in the intracellular level of succinate, an intermediate of the TCA cycle, by

1,25(OH)$_2$D treatment in the MCF10A-*ras* cells, but not in MCF10A cells, compared to vehicle (Figure 4D). The latter provides further support of the overall reduction in TCA cycle activity in response to 1,25(OH)$_2$D in cells during early progression to tumors. In contrast, mRNA expression of pyruvate dehydrogenase kinase 1 (PDK1) (Figure 4E), the inhibiting kinase of PDH that regulates the flux of pyruvate into the TCA cycle, was not altered by 1,25(OH)$_2$D in MCF10A or MCF10A-*ras* cells, suggesting that the reduced PDH activity and flux of glucose into the TCA cycle induced by 1,25(OH)$_2$D may not be mediated through upregulation of PDK1.

4. Discussion

Alteration in cellular glucose metabolism is a signature characteristic of tumor cells which drives cell proliferation by increasing bioenergetics and biosynthesis, maintaining redox potential, and via initiation of signal transduction controlled by changes in cellular metabolism [11, 36, 37]. Interventions that target metabolic pathways are now emerging as potential preventive or therapeutic approaches for the treatment of cancers [18, 19, 38, 39]. In the current study, the effects of 1,25(OH)$_2$D on cellular energy metabolism were explored in untransformed and H-*ras* oncogene transfected MCF10A cells, a human breast epithelial cell model for studying early mammary carcinogenesis. The results support the hypothesis that 1,25(OH)$_2$D reduces the glucose addiction of cells in progression to cancer, as a consequence of the shift in glucose metabolism towards reduced glycolysis and lactate production (reversal of the classic Warburg effect) as well as reduced TCA cycle activity in *H-ras* transfected MCF10A cells, suggesting a preventive effect of 1,25(OH)$_2$D on glucose utilization for rapid cell proliferation during breast cancer progression. To our knowledge, these results are the first to show that 1,25(OH)$_2$D regulates cellular glucose metabolism which may be a potential mechanism for preventing early breast cancer progression.

Previous studies suggested that activity of the activated K-*ras* gene alone may lead to an increase in glycolysis in mouse and human cells [22], similar to that seen in cancer cells [11, 40]. Results from our laboratory support these results. The MCF10A-*ras* cells, which represent an initiation stage of tumor progression, show changes in several energy status parameters that are characteristic of tumors, including the increased glucose uptake (by 2.1 fold, $P<0.01$) [41] and lactate accumulation (by 2.4 fold, $P<0.05$, data not shown), which is consistent with the Warburg effect [40, 42], supporting the hypothesis that very early changes in energy status may occur during cancer progression in the presence of the H-*ras* oncogene. The current study suggests that 1,25(OH)$_2$D may reverse the alterations in glucose metabolism during early breast cancer progression mediated by the H-*ras* oncogene. One of the outcomes for the altered glucose metabolism by 1,25(OH)$_2$D was the reduced glucose addiction via reducing G1 cell cycle arrest at glucose restriction. It has been suggested that part of the chemopreventive effects of 1,25(OH)$_2$D against cancer is mediated by G1 cell-cycle arrest, as a result of the upregulation of proteins suppressing cyclin-dependent kinase activity [43-45]. Consistently, the current study showed that 1,25(OH)$_2$D induced the G1 cell cycle arrest of MCF10A-*ras* cells but prevented the increase in G1 arrest (Figure 1B) at glucose restriction, suggesting 1,25(OH)$_2$D may reduce the glucose addiction of MCF10A-*ras* cells through the regulation of G1 cell cycle arrest.

Results suggesting a reduction in glycolysis by $1,25(OH)_2D$ are supported by the reduced flux of glucose to 3-phosphoglycerate by $1,25(OH)_2D$ in MCF10A and MCF10A-*ras* cells respectively. In the MCF10A-*ras* cells, $1,25(OH)_2D$ was shown to reduce lactate production, and a reduction of intracellular lactate levels, as well as a reduction in lactate dehydrogenase activity. $1,25(OH)_2D$-induced reduction in TCA cycle activity was observed as reduced glucose flux to acetyl-coA and to oxaloacetate in the MCF10A and MCF10A-*ras* cells, respectively. It is also intriguing that one of the glycolytic intermediates, PEP, was increased by $1,25(OH)_2D$ in the MCF10A-*ras* cells. One mechanism that may contribute to the accumulation of PEP may be due to the reduced activity of the enzyme downstream of this metabolite in the glycolytic pathway, PK. PK regulates the rate-limiting and final step of glycolysis, the conversion of PEP to pyruvate. The M2 isoform (PKM2) is a critical enzyme expressed predominantly in tumor tissues that promotes aerobic glycolysis [35]. The accumulation of PEP suggests a potentially decreased activity of PKM2 by $1,25(OH)_2D$. However, the mRNA expression of PKM2 was not different in vehicle and $1,25(OH)_2D$ treated MCF10A and MCF10A-*ras* cells (Figure 2H); and neither was the total activity of PK enzyme (Figure 2I), suggesting that accumulation of PEP is not a result of reduced PK activity by $1,25(OH)_2D$. Regulation of the activity of other enzymes in hexogenesis, glycolysis or flux into the TCA cycle may contribute to the increased accumulation of PEP mediated by $1,25(OH)_2D$. There are differential effects of $1,25(OH)_2D$ on energy metabolism and cell growth in the untransformed and *ras* oncogene transformed MCF10A cells. Overall, our results suggest that $1,25(OH)_2D$ has a greater effect on metabolic parameters in the MCF10A-*ras* cells than in MCF10A cells, which may contribute to the growth inhibitory effects in different glucose concentrations (Figure 1A lower panel). Although there are changes in some of the metabolic parameters by $1,25(OH)_2D$ in MCF10A cells (Figure 2, 4), there are no changes in the biological consequences (growth) in these cells (Figure 1A upper panel). These differences in quantitative impact of $1,25(OH)_2D$ may suggest that the effects in MCF10A cells were not great enough to lead to a change with respect to growth in different glucose concentration. Further investigations are needed to understand how the changes in metabolic parameters contribute to the biological consequences such as growth and glucose dependence.

Overall, the results of the current study support our hypothesis that $1,25(OH)_2D$ regulates the metabolic reprogramming during early breast cancer progression. Specifically, $1,25(OH)_2D$ reduces cell glucose addiction, shifts glucose utilization towards reduced glycolysis and lactate production as well as reduced flux through the TCA cycle in *H-ras* transformed MCF10A breast epithelial cells. To our knowledge, this is the first study to demonstrate that $1,25(OH)_2D$ regulates cellular energy metabolism in a model of early breast cancer progression. These results indicate that vitamin D, as a potential chemopreventive agent, has multiple functions during cancer progression. Acquiring a better understanding of vitamin D regulation of glucose metabolism during cancer progression should allow the identification of its targeted regulatory points in the metabolic pathways and its interaction with oncogenes such as *ras*, so as to contribute to the development of effective strategies for breast cancer prevention.

Acknowledgments

This work was supported by the National Institutes of Health, National Cancer Institute R25CA128770 (D. Teegarden) Cancer Prevention Internship Program (W. Zheng) administered by the Oncological Sciences Center and the Discovery Learning Research Center at Purdue University and by NIH 1R01GM085291 (D. Raftery).

Abbreviations

1,25(OH)$_2$D	1,25-dihydroxyvitamin D
VDR	vitamin D receptor
TCA cycle	tricarboxylic acid cycle
LDH	lactate dehydrogenase
PDH	pyruvate dehydrogenase
PDK	pyruvate dehydrogenase kinase
GLUT1	glucose transporter 1
HK2	hexokinase 2
PGK1	phosphoglycerate kinase1
PEP	phosphoenolpyruvate
PK	pyruvate kinase
PBS	phosphate buffered saline
MTT	3-(4, 5-dimethylthiazolyl-2)-2, 5-diphenyltetrazolium bromide
NMR	nuclear magnetic resonance spectroscopy
MS	mass spectrometry

Reference List

1. Stebbing J, Ngan S. Breast cancer (metastatic). Clin Evid. 2010 (Online.) 2010.
2. Garland CF, Gorham ED, Mohr SB, Grant WB, Giovannucci EL, Lipkin M, Newmark H, Holick MF, Garland FC. Vitamin D and prevention of breast cancer: pooled analysis. J Steroid Biochem. Mol Biol. 2007; 103:708–711.
3. Garland FC, Garland CF, Gorham ED, Young JF. Geographic variation in breast cancer mortality in the United States: a hypothesis involving exposure to solar radiation. Prev. Med. 1990; 19:614–622. [PubMed: 2263572]
4. Hiatt RA, Krieger N, Lobaugh B, Drezner MK, Vogelman JH, Orentreich N. Prediagnostic serum vitamin D and breast cancer. J. Natl. Cancer Inst. 1998; 90:461–463. [PubMed: 9521171]
5. Janowsky EC, Lester GE, Weinberg CR, Millikan RC, Schildkraut JM, Garrett PA, Hulka BS. Association between low levels of 1,25-dihydroxyvitamin D and breast cancer risk. Public Health Nutr. 1999; 2:283–291. [PubMed: 10512563]
6. Lappe JM, Travers-Gustafson D, Davies KM, Recker RR, Heaney RP. Vitamin D and calcium supplementation reduces cancer risk: results of a randomized trial. Am. J Clin Nutr. 2007; 85:1586–1591. [PubMed: 17556697]
7. Garland CF, Garland FC, Gorham ED, Lipkin M, Newmark H, Mohr SB, Holick MF. The role of vitamin D in cancer prevention. Am. J. Public Health. 2006; 96:252–261. [PubMed: 16380576]
8. Fleet JC, DeSmet M, Johnson R, Li Y. Vitamin D and cancer: a review of molecular mechanisms. Biochem. J. 2012; 441:61–76. [PubMed: 22168439]

9. Krishnan AV, Feldman D. Mechanisms of the anti-cancer and anti-inflammatory actions of vitamin D. Annu. Rev. Pharmacol. Toxicol. 2011; 51:311–336. [PubMed: 20936945]
10. WARBURG O. On the origin of cancer cells. Science. 1956; 123:309–314. [PubMed: 13298683]
11. Vander Heiden MG, Cantley LC, Thompson CB. Understanding the Warburg effect: the metabolic requirements of cell proliferation. Science. 2009; 324:1029–1033. [PubMed: 19460998]
12. Gillies RJ, Robey I, Gatenby RA. Causes and consequences of increased glucose metabolism of cancers. J Nucl. Med. 49 Suppl. 2008; 2:24S–42S.
13. Jones RG, Thompson CB. Tumor suppressors and cell metabolism: a recipe for cancer growth. Genes Dev. 2009; 23:537–548. [PubMed: 19270154]
14. Kim JW, Dang CV. Cancer's molecular sweet tooth and the Warburg effect. Cancer Res. 2006; 66:8927–8930. [PubMed: 16982728]
15. Feron O. Pyruvate into lactate and back: from the Warburg effect to symbiotic energy fuel exchange in cancer cells. Radiother. Oncol. 2009; 92:329–333. [PubMed: 19604589]
16. Spitz DR, Sim JE, Ridnour LA, Galoforo SS, Lee YJ. Glucose deprivation-induced oxidative stress in human tumor cells. A fundamental defect in metabolism? Ann. N. Y. Acad. Sci. 2000; 899:349–362. [PubMed: 10863552]
17. Caro-Maldonado A, Tait SW, Ramirez-Peinado S, Ricci JE, Fabregat I, Green DR, Munoz-Pinedo C. Glucose deprivation induces an atypical form of apoptosis mediated by caspase-8 in Bax-, Bak-deficient cells. Cell Death. Differ. 2010; 17:1335–1344. [PubMed: 20203689]
18. Cao X, Fang L, Gibbs S, Huang Y, Dai Z, Wen P, Zheng X, Sadee W, Sun D. Glucose uptake inhibitor sensitizes cancer cells to daunorubicin and overcomes drug resistance in hypoxia. Cancer Chemother. Pharmacol. 2007; 59:495–505. [PubMed: 16906425]
19. Pelicano H, Martin DS, Xu RH, Huang P. Glycolysis inhibition for anticancer treatment. Oncogene. 2006; 25:4633–4646. [PubMed: 16892078]
20. Pylayeva-Gupta Y, Grabocka E, Bar-Sagi D. RAS oncogenes: weaving a tumorigenic web. Nat. Rev. Cancer. 2011; 11:761–774. [PubMed: 21993244]
21. Kiaris H, Spandidos D. Mutations of ras genes in human tumors (review). Int. J Oncol. 1995; 7:413–421. [PubMed: 21552855]
22. Gaglio D, Metallo CM, Gameiro PA, Hiller K, Danna LS, Balestrieri C, Alberghina L, Stephanopoulos G, Chiaradonna F. Oncogenic K-Ras decouples glucose and glutamine metabolism to support cancer cell growth. Mol. Syst. Biol. 2011; 7:523. [PubMed: 21847114]
23. Taber LM, Adams LS, Teegarden D. Mechanisms of nuclear vitamin D receptor resistance in Harvey-ras-transfected cells. J Nutr. Biochem. 2008
24. Solomon C, White JH, Kremer R. Mitogen-activated protein kinase inhibits 1,25-dihydroxyvitamin D3-dependent signal transduction by phosphorylating human retinoid X receptor alpha. J Clin. Invest. 1999; 103:1729–1735. [PubMed: 10377179]
25. Solomon C, Kremer R, White JH, Rhim JS. Vitamin D resistance in RAS-transformed keratinocytes: mechanism and reversal strategies. Radiat. Res. 2001; 155:156–162. [PubMed: 11121228]
26. Soule HD, Maloney TM, Wolman SR, Peterson WD Jr. Brenz R, McGrath CM, Russo J, Pauley RJ, Jones RF, Brooks SC. Isolation and characterization of a spontaneously immortalized human breast epithelial cell line, MCF-10. Cancer Res. 1990; 50:6075–6086. [PubMed: 1975513]
27. Asiago VM, Alvarado LZ, Shanaiah N, Gowda GA, Owusu-Sarfo K, Ballas RA, Raftery D. Early detection of recurrent breast cancer using metabolite profiling. Cancer Res. 2010; 70:8309–8318. [PubMed: 20959483]
28. Gowda GA, Zhang S, Gu H, Asiago V, Shanaiah N, Raftery D. Metabolomics-based methods for early disease diagnostics. Expert. Rev. Mol. Diagn. 2008; 8:617–633. [PubMed: 18785810]
29. Zhang S, Liu L, Steffen D, Ye T, Raftery D. Metabolic Profiling of Gender: SPME/GC-MS and 1H NMR Analysis of Urine. Metabolomics. 2012; 8:323–334.
30. Brauman JI. Least square analysis and simplification of multi-isotope mass spectra. Anal Chem. 1966:607–610.

31. Bequette BJ, Sunny NE, El-Kadi SW, Owens SL. Application of stable isotopes and mass isotopomer distribution analysis to the study of intermediary metabolism of nutrients. J Anim Sci. 2006; 84(Suppl):E50–E59. [PubMed: 16582092]
32. Fernandez CA, Des RC. Modeling of liver citric acid cycle and gluconeogenesis based on 13C mass isotopomer distribution analysis of intermediates. J. Biol. Chem. 1995; 270:10037–10042. [PubMed: 7730305]
33. McLamore ES, Shi J, Jaroch D, Claussen JC, Uchida A, Jiang Y, Zhang W, Donkin SS, Banks MK, Buhman KK, Teegarden D, Rickus JL, Porterfield DM. A self referencing platinum nanoparticle decorated enzyme-based microbiosensor for real time measurement of physiological glucose transport. Biosens. Bioelectron. 2010; 26:2237–2245. [PubMed: 20965716]
34. McLamore ES, Porterfield DM. Non-invasive tools for measuring metabolism and biophysical analyte transport: self-referencing physiological sensing. Chem. Soc. Rev. 2011; 40:5308–5320. [PubMed: 21761069]
35. Christofk HR, Vander Heiden MG, Harris MH, Ramanathan A, Gerszten RE, Wei R, Fleming MD, Schreiber SL, Cantley LC. The M2 splice isoform of pyruvate kinase is important for cancer metabolism and tumour growth. Nature. 2008; 452:230–233. [PubMed: 18337823]
36. Metallo CM, Vander Heiden MG. Metabolism strikes back: metabolic flux regulates cell signaling. Genes Dev. 2010; 24:2717–2722. [PubMed: 21159812]
37. Locasale JW, Cantley LC. Metabolic flux and the regulation of mammalian cell growth. Cell Metab. 2011; 14:443–451. [PubMed: 21982705]
38. Michelakis ED, Sutendra G, Dromparis P, Webster L, Haromy A, Niven E, Maguire C, Gammer TL, Mackey JR, Fulton D, Abdulkarim B, McMurtry MS, Petruk KC. Metabolic modulation of glioblastoma with dichloroacetate. Sci. Transl. Med. 2010; 2:31ra34.
39. Vander Heiden MG, Christofk HR, Schuman E, Subtelny AO, Sharfi H, Harlow EE, Xian J, Cantley LC. Identification of small molecule inhibitors of pyruvate kinase M2. Biochem. Pharmacol. 2010; 79:1118–1124. [PubMed: 20005212]
40. Gatenby RA, Gillies RJ. Why do cancers have high aerobic glycolysis? Nat. Rev. Cancer. 2004; 4:891–899. [PubMed: 15516961]
41. Zheng W, McLamore ES, Porterfield DM, Donkin SS, Teegarden D. Effect of 1,25 dihydroxyvitamin D on energy metabolism in MCF10A breast epithelial cells. The FASEB Journal. 2011; 25(235.1) Ref Type: Abstract.
42. Cook CC, Kim A, Terao S, Gotoh A, Higuchi M. Consumption of oxygen: a mitochondrial-generated progression signal of advanced cancer. Cell Death. Dis. 2012; 3:e258. [PubMed: 22258408]
43. Scaglione-Sewell BA, Bissonnette M, Skarosi S, Abraham C, Brasitus TA. A vitamin D3 analog induces a G1-phase arrest in CaCo-2 cells by inhibiting cdk2 and cdk6: roles of cyclin E, p21Waf1, and p27Kip1. Endocrinology. 2000; 141:3931–3939. [PubMed: 11089522]
44. Jensen SS, Madsen MW, Lukas J, Binderup L, Bartek J. Inhibitory effects of 1alpha,25-dihydroxyvitamin D(3) on the G(1)-S phase-controlling machinery. Mol. Endocrinol. 2001; 15:1370–1380. [PubMed: 11463860]
45. Lamprecht SA, Lipkin M. Chemoprevention of colon cancer by calcium, vitamin D and folate: molecular mechanisms. Nat. Rev. Cancer. 2003; 3:601–614. [PubMed: 12894248]

Highlights

► $1,25(OH)_2D$ reduces glucose addiction of *ras*-oncogene transformed MCF10A breast epithelial cells.

► $1,25(OH)_2D$ reduces glucose utilization in glycolysis, lactate production and the TCA cycle.

► Regulation of cellular glucose metabolism is a novel mechanism for $1,25(OH)_2D$ action in cancer prevention.

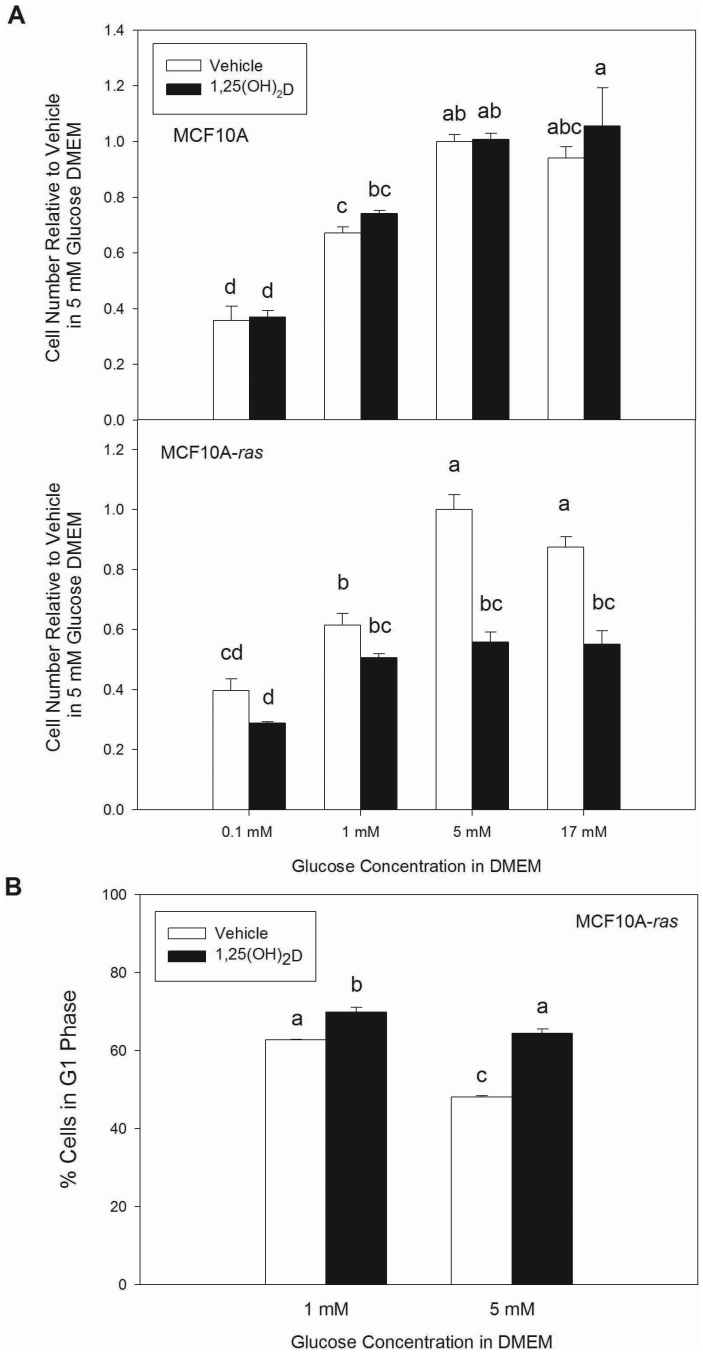

Figure 1. 1,25(OH)$_2$D reduces glucose addiction

MCF10A and MCF10A-*ras* cells were treated with vehicle or 1,25(OH)$_2$D (10nM) for 4 days before analysis. Cells were switched from media containing 5 mM glucose to the indicated glucose levels for the last 24 hours. **A.** Relative amount of MCF10A and MCF10A-*ras* cells compared to vehicle treated cells in 5 mM glucose media assessed by MTT assay. B. Percentage of MCF10A-*ras* cells arrested in G1 cell cycle, analyzed by flow cytometry. Groups with the same letters are not significantly different ($P < 0.05$).

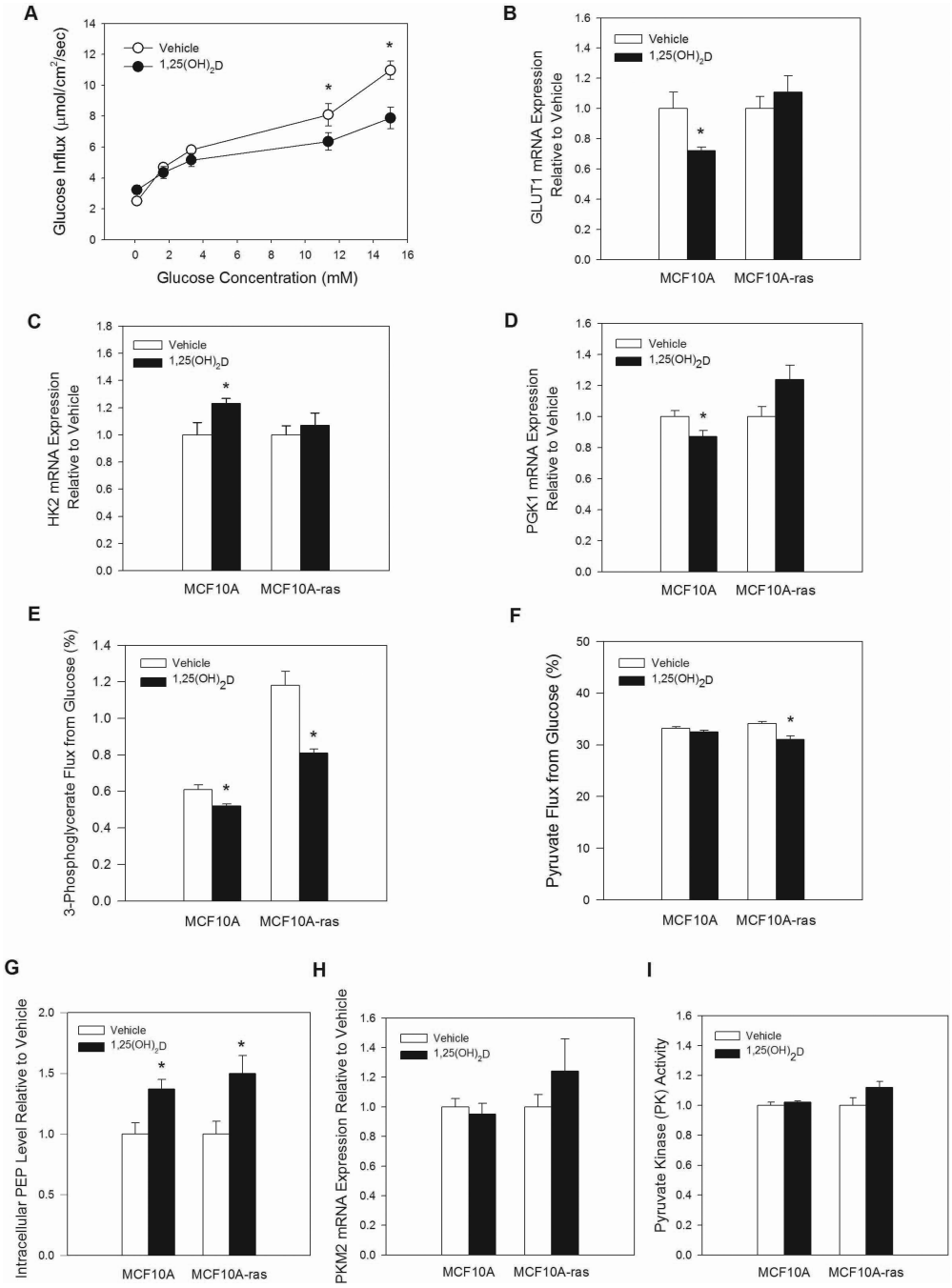

Figure 2. 1,25(OH)$_2$D reduces glucose uptake and aerobic glycolysis

MCF10A and MCF10A-*ras* cells were treated with vehicle or 1,25(OH)$_2$D (10nM) for 4 days before measurement or harvest. **A.** Glucose influx at the cell membrane (μmol/cm^2/sec) in response to increasing doses of added glucose in the media in MCF10A-*ras* cells (n = 4). The mRNA expression is shown for GLUT1 (**B**), HK2 (**C**), and PGK1 (**D**) relative to vehicle in each cell type (n = 3). Flux contributions of $^{13}C_6$-labeled glucose to 3-phosphoglycerate (**E**) and pyruvate (**F**) are shown in percent metabolite flux from glucose (n = 4). **G.** Intracellular levels of phosphoenolpyruvate (PEP) relative to vehicle treatment in each cell type (n = 4). **H.** The mRNA expression of PKM2 relative to vehicle in each cell type (n = 3). **I.** The enzyme activity of total PK relative

to vehicle in each cell type (n = 3). Results are expressed as mean ± SEM. An asterisk (*) indicates a significant difference between vehicle and $1,25(OH)_2D$ treatments within the same cell type ($P < 0.05$).

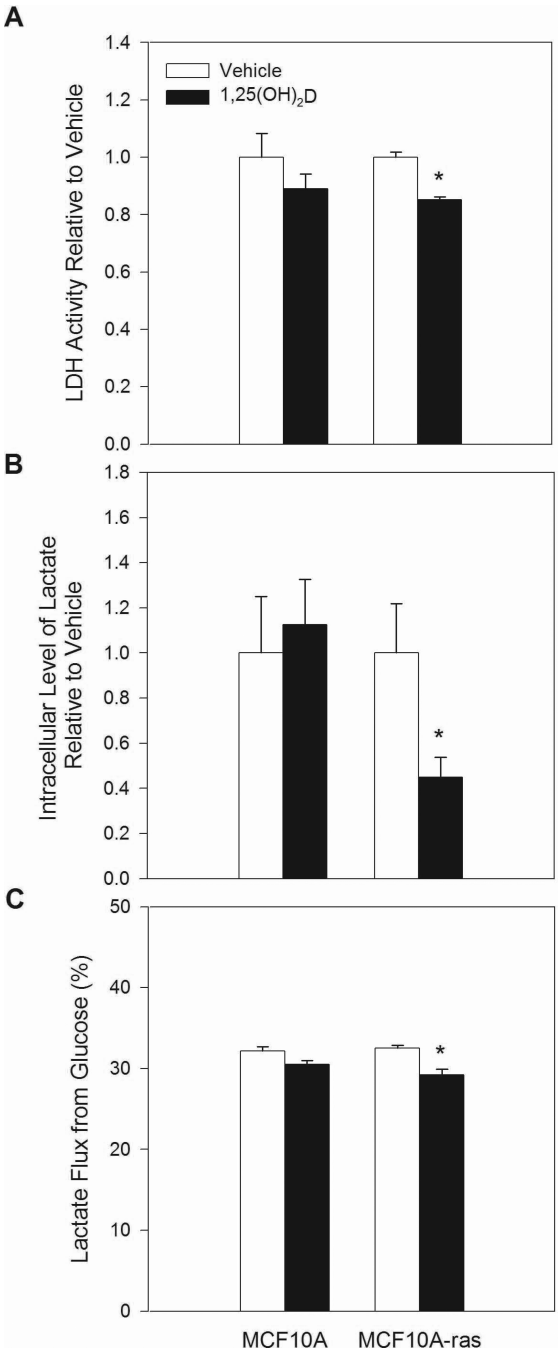

Figure 3. 1,25(OH)$_2$D reduces lactate production

MCF10A and MCF10A-*ras* cells were treated with vehicle or 1,25(OH)$_2$D (10nM) for 4 days before harvest. **A.** Lactate dehydrogenase (LDH) activity relative to vehicle treatment in the same cell type (n = 3). **B.** Intracellular levels of lactate relative to vehicle treatment in each cell type (n = 4). **C.** Flux contributions of $^{13}C_6$-labeled glucose to lactate shown in percent metabolite flux from glucose (n = 4). Results are expressed as mean ± SEM. An asterisk (*) indicates a significant difference between vehicle and 1,25(OH)$_2$D treatments within the same cell type ($P < 0.05$).

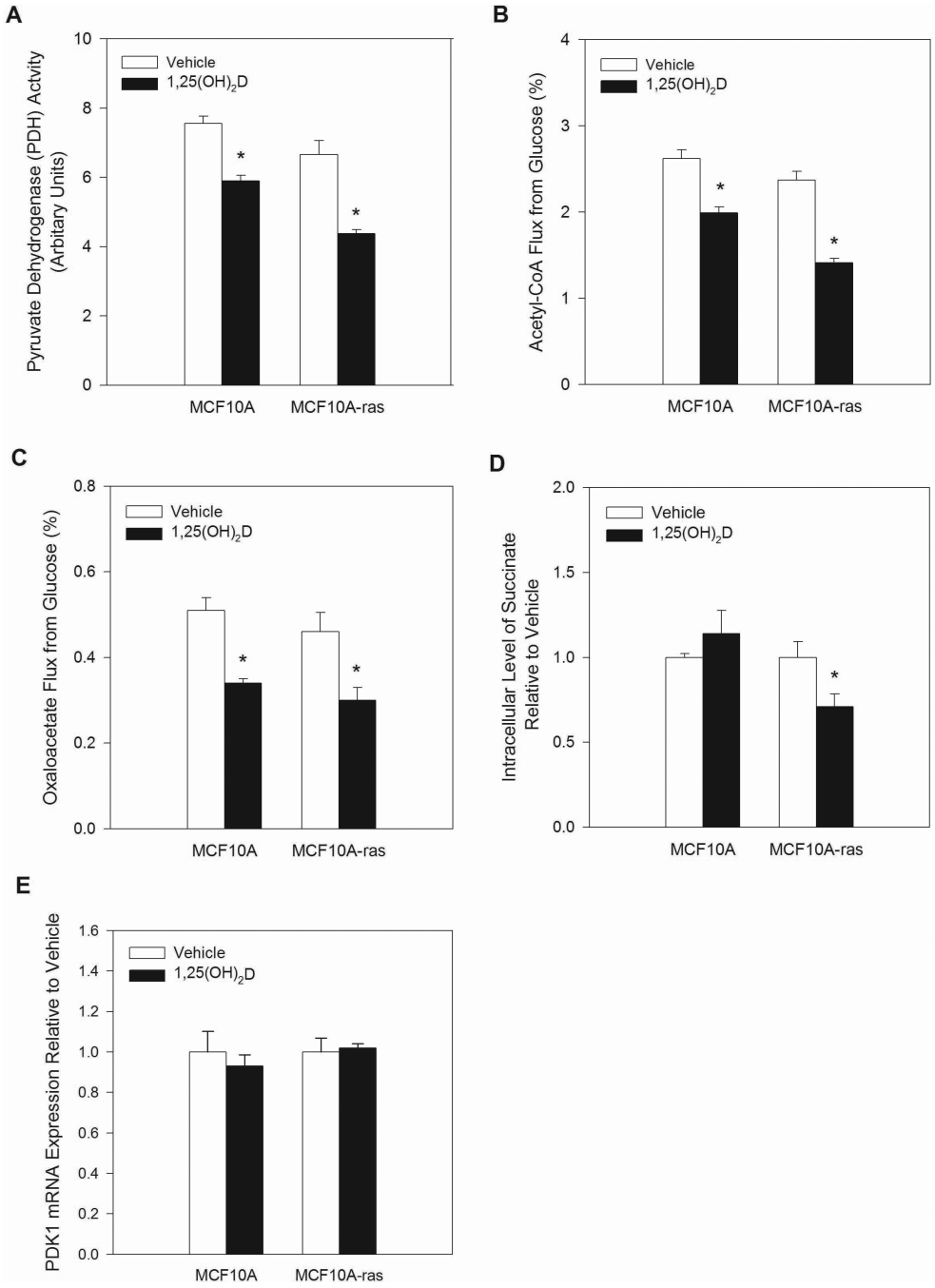

Figure 4. 1,25(OH)$_2$D reduces TCA cycle activity

MCF10A and MCF10A-*ras* cells were treated with vehicle or 1,25(OH)$_2$D (10nM) for 4 days before measurement or harvest. Flux contributions of $^{13}C_6$-labeled glucose to **A.** acetyl-CoA and **B.** oxaloacetate shown in percent metabolite flux from glucose. **C**. Pyruvate dehydrogenase activity shown in arbitrary units (n = 4). **D.** Intracellular levels of succinate relative vehicle in each cell type (n = 4). **E.** The mRNA expression of PDK1 relative to vehicle in each cell type (n = 3). Results are expressed as mean ± SEM. An asterisk (*) indicates a significant difference between vehicle and 1,25(OH)$_2$D treatments within the same cell type ($P < 0.05$).

Table 1

Primers used in QPCR analysis of gene expression.

Genes	Primer information
GLUT1	Forward: 5'- TATCGTCAACACGGCCTTCACTGT-3' Reverse: 5'- CACAAAGCCAAAGATGGCCACGAT-3'
HK2	Forward: 5'- CTGCAGCGCATCAAGGAGAACAAA-3' Reverse: 5'- ACGGTCTTATGTAGACGCTTGGCA-3'
PGK1	Forward: 5'- TCACTCGGGCTAAGCAGATTGTGT-3' Reverse: 5'- CGTGTTCCATTTGGCACAGCAAGT-3'
PKM2	Forward: 5'-ATTATTTGAGGAACTCCGCCGCCT-3' Reverse: 5'- CATTCATGGCAAAGTTCACCCGGA-3'
PDK1	Forward: 5'- TCATGTCACGCTGGGTAATGAGGA-3' Reverse: 5'- AACACGAGGTCTTGGTGCAGTTGA-3'
18S	Forward: 5'-TTAGAGTGTTCAAAGCAGGCCCGA-3' Reverse: 5'-TCTTGGCAAATGCTTTCGCTCTGG-3'